Tcvetkova, Svetlana; Asadchy, Viktar; Tretyakov, Sergei

Scanning properties of novel metasurface-based reflector antennas

Published in:
Proceedings of the 46th European Microwave Conference Proceedings, EuMC 2016

DOI:
10.1109/EuMC.2016.7824372

Published: 01/01/2016

Document Version
Peer-reviewed accepted author manuscript, also known as Final accepted manuscript or Post-print

Please cite the original version:
Tcvetkova, S., Asadchy, V., & Tretyakov, S. (2016). Scanning properties of novel metasurface-based reflector antennas. In *Proceedings of the 46th European Microwave Conference Proceedings, EuMC 2016* (pp. 433-436). Article 7824372 (European Microwave Conference). European Microwave Association. https://doi.org/10.1109/EuMC.2016.7824372

Scanning properties of novel metasurface based reflector antennas

Svetlana Tcvetkova, Viktar Asadchy, and Sergei Tretyakov
School of Electrical Engineering, Aalto University, Finland FI-00073
Email: svetlana.tcvetkova@aalto.fi, viktar.asadchy@aalto.fi

***Abstract*—We investigate beam scanning by lateral feed displacement in novel metasurface based reflector antennas with extremely short focal distances which emulate a cylindrical lens in reflection. Two reciprocal cases of illumination are explored: illumination by a plane wave (focusing to a spot) and illumination by a source of cylindrical waves from the focal point (plane wave in reflection). For the former case, the power density distribution of the reflected waves from the metamirror are studied numerically for scanned beam angles up to 10° from the normal for two f/D-ratios. For the latter, electric field distributions of the waves reflected from the antenna are explored numerically and experimentally for defocusing angles up to 16°. The results show that despite extremely small focal distances, the scanning ability of metamirrors is similar to that of comparable reflectarrays. In addition to offering a possibility to realize extremely small focal distances, metamirror antennas are practically invisible for any radiation beyond the operating frequency range.**

I. Introduction

Beam scanning ability of reflector antennas is an important feature for radar technologies and other applications. For passive reflectors, beam scanning or producing multiple beams can be accomplished through the lateral feed displacement (Fig. 1).

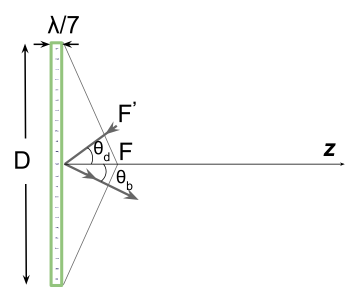

Fig. 1. Lateral feed displacement in metasurface based reflector.

Geometrical parameters of reflectors are usually defined by the ratio between the focal length and the diameter (f/D) or by the subtended angle θ_0 (for example, that equals to $\theta_0 = \tan^{-1}(0.5D/f)$ for reflectarrays). When the feed is laterally displaced from the focal point of the reflector at a defocusing angle θ_d, the scanned beam is deflected at the angle θ_b (see Fig. 1). The beam deviation factor, which can be described as $BDF = \theta_b/\theta_d$ is always less than unity for all known reflector structures.

Conventional reflector antennas that allow feed-displacement scanning can be classified into parabolic reflectors and reflectarrays. Recently, a new type of reflector antennas was introduced, based on metasurfaces with deeply sub-wavelength thickness [1], [2]. The structure of these reflecting metasurfaces can be considered as a novel reflectarray structure, which excludes a continuous reflecting surface (ground plane) that, however, does not compromise the high performance of the reflector antenna in the operational frequency band. These new reflector antennas, called *metamirrors,* are practically transparent and invisible for any radiation with frequencies beyond the desired operational band. Such a unique functionality can be of paramount importance for many different applications, such as reflector antennas for satellites incorporated with the solar panels (more than 95% of solar energy is expected to be delivered to the panels through the antenna). Another exciting potential application of metamirrors is creating multi-functional and multi-frequency antenna arrays which combine several independent thin layers operating at different frequencies and performing different functionalities (with the overall thickness still not exceeding the wavelength) [3]. Due to their deeply sub-wavelength constituent elements, metamirrors demonstrate an ability to confine incident energy at an extremely short focal distance, less than the operating wavelength.

Properties of conventional reflector antennas when the beam-scanning performance is accomplished by lateral displacement of the feed from the focal point are well known. Traditionally, such antennas are designed for limited scan angles because of phase errors which can cause loss in the gain and degradation of the beam [4]. However, so far, the scanning characteristics of metamirrors have not been studied. It could be expected that metamirrors with sub-wavelength focal distances would experience the problem of extremely high beam degradation when the feed is laterally displaced from the focal point. For example, in reception regime it would appear as severe distortions of the focusing ability when even a slight deviation of the incidence angle from the target occurred. The goal of this work is to investigate beam-scanning properties of novel metamirrors with a sub-wavelength focal distance. Example of metamirrors emulating cylindrical lenses in reflection regime are considered for two cases of metasufrace illumination. One of them is a plane wave illumination and another is illumination by a source of cylindrical waves from the focal point. We demonstrate, both numerically and experimentally, that despite of the sub-wavelength focal distance, the metasurface based reflectors possess quite acceptable scanning properties suitable for many applications.

II. Scanning properties of metamirror arrays emulating a cylindrical lens in reflection

A. Ground-free reflector and its operation principles

The operation mechanism of metamirrors is radically different from that of any type of known reflector antennas. In contrast to conventional reflectors, a metamirror does not include any ground plane and generally represents a planar array of sub-wavelength sized elements embedded for mechanical support in a low-permittivity dielectric material (see Fig. 2).

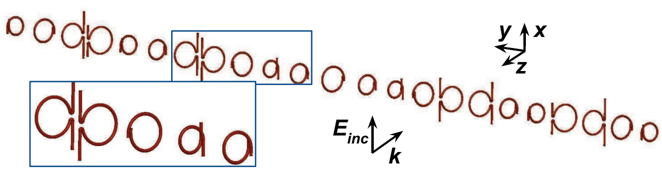

Fig. 2. Metamirror formed by a single row of specifically shaped copper elements imitating a cylindrical lens in reflection.

In conventional reflectors, such as reflectarrays, the high reflection amplitude is achieved through a continuous ground plane. Since metamirrors lack of a ground plane, their elements perform double functionality. First, they radiate a unit-magnitude wave in the backward direction $E_{\rm back} = e^{j\phi} E_{\rm inc}$ with the prescribed non-uniform phase distribution. Second, in the forward direction, they scatter a plane wave (with a uniform phase) which is opposite to the phase of the incident wave $E_{\rm forw} = -E_{\rm inc}$ to ensure their destructive interference and zero transmission. Such asymmetric scattering properties [2] require both electric and magnetic currents induced in the elements. It was shown in [1] that a more effective and practical way to accomplish this condition in ground-free reflector is based on the use of small scatterers comprising both induced electric and magnetic currents in a single element. Such magnetoelectric elements comprise electrically polarizable straight wires which are connected to magnetically polarizable wire loops (see Fig. 2). Changing the ratio between the length of the straight wires and the diameter of the loop, it is possible to design an arbitrary phase from 0 to 2π of the backscattered wave from the element.

B. Metamirror under illumination of a plane wave

We consider two metamirror arrays (Fig. 2) composed of 23 (long array) and 11 (short array) specifically shaped sub-wavelength copper elements embedded in a dielectric support with $\epsilon_r = 1.03$ and $\tan\delta = 0.0001$. The metamirrors are infinite and periodical along the x-axis. Both arrays are axially symmetric with respect to the z-axis. Each element is located in a unit cell with the size of $a = 15$ mm. The thickness of the metamirror is approximately $\lambda/7$ at the operating frequency 5 GHz. The sub-wavelength focal distance of such metamirrors (0.65λ) implies very small focal length to diameter ratios and large subtended angles (for long array $f/D = 0.12$ and $\theta_0 = 77^\circ$, for short array $f/D = 0.23$ and $\theta_0 = 65^\circ$). The scanning properties of these reflectors were studied numerically.

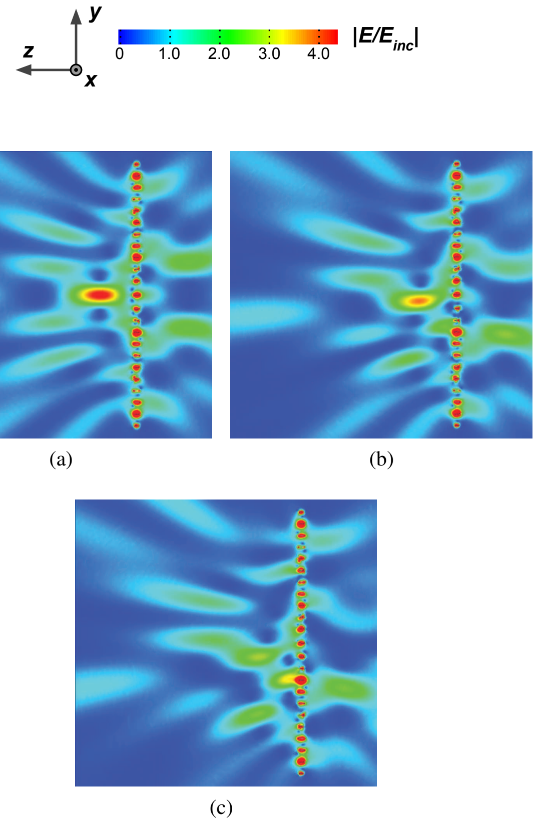

Fig. 3. Simulated results of the power density distribution of the transmitted (in the $-z$ half-space) and reflected (in the $+z$ half-space) waves normalized to the incident power density for the metamirror with $f/D = 0.12$. The metamirror is located at $z = 0$. (a) Normal incidence. (b) Oblique incidence at an angle $\theta_b = 5^\circ$ from the $+z$-axis (counted towards the $+y$-direction). (c) Oblique incidence at an angle $\theta_b = 10^\circ$. The incident wave illuminates the metasurface from the $+z$-direction.

The metamirrors were illuminated by the obliquely incident plane waves and the displacements of the focal spot in reflection were studied. The angle of incidence θ_b deviated from 0 to 10 degrees from the normal ($+z$-direction). The power density distributions of the transmitted and the reflected waves, normalized to the incident power density, are plotted for different deviation angles in Fig. 3 and Fig. 4 for the metamirrors with $f/D = 0.12$ and $f/D = 0.23$, respectively. The numerical data are summarized in Table I.

The plots show that the short metamirror at oblique angles efficiently focuses reflected waves for a moderate deflection of the incidence. However, for the long metamirror the focusing effect vanishes for oblique incidence at angles exceeding 5 degrees from the normal. This can be explained by the increasing phase errors in the inclusions occurring in the long sample. By comparing these two metamirrors with different sizes, one can conclude that the longer array, the higher power gain in the focal spot. However, the number of phase overlaps increases with the subtended angle value increase (or

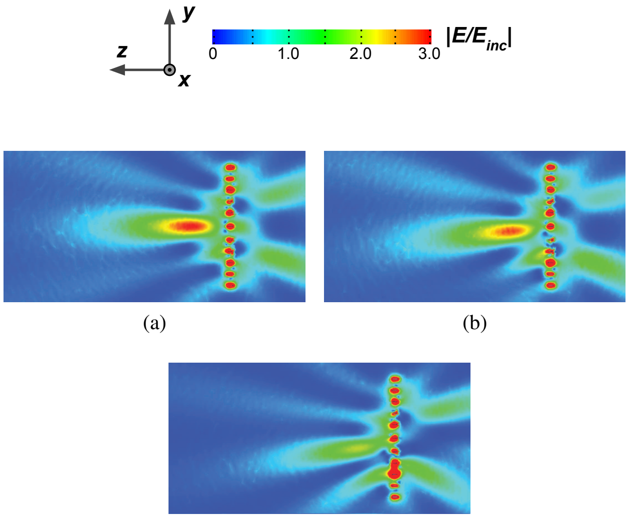

(a) (b)

(c)

Fig. 4. Simulated results of the power density distribution of the transmitted (in the $-z$ half-space) and reflected (in the $+z$ half-space) waves normalized to the incident power density for the metamirror with $f/D = 0.23$. The metamirror is located at $z = 0$. (a) Normal incidence. (b) Oblique incidence at an angle $\theta_b = 5°$ from the $+z$-axis (counted towards the $+y$-direction). (c) Oblique incidence at an angle $\theta_b = 10°$.

Declination of the incident wave from the normal θ_b, deg	Defo - cusing angle for long/short arrays θ_d, deg	Power gain in the shifted focal spot for long/ short arrays	Power gain in the positions of the initial focal spot for long/ short arrays	Beam deviation factor BDF for long/ short arrays
0	0 / 0	4.3 / 3	4.3 / 3	-
5	9 / 7.5	3.6 / 2.8	2.7 /	0.55 / 0.66
10	17.7 / 15.2	2.6 / 2	0.6 /	0.56 / 0.65

TABLE I
FOCAL SPOT DISPLACEMENT FOR OBLIQUE ILLUMINATION

reduction of f/D ratio), because the path difference between different points of the metamirror and the feed can consist of a greater number of wavelengths. In addition, it can be seen that the gain in the shifted focal spot becomes slightly smaller when the incidence angle increases, as expected. Taking into account the extremely short focal distance, the ability of the studied metamirror to collect electromagnetic energy can be considered as remarkable.

C. Metamirror under illumination by a source of cylindrical waves placed in the focal point

In this section we consider reciprocally opposite case of illumination. A source of cylindrical waves (along the x-axis) is positioned in the focal point of the metamirror (only long array with $f/D = 0.12$ is in consideration). This structure, operating as a cylindrical lens, reflect a collimated plane wave (a beam in the finite case). When the source of cylindrical waves is displaced from the focal point, the reflected wave is

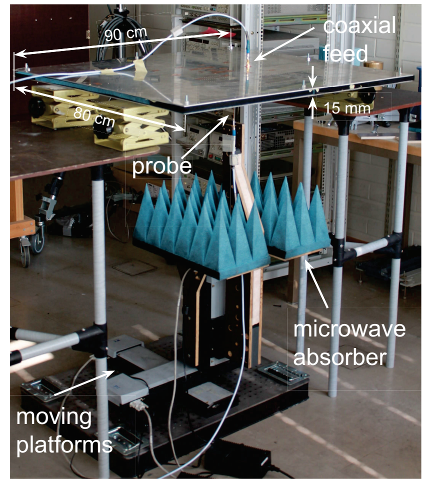

Fig. 5. Experimental set-up including moving platforms, a coaxial probe, feed antennas and a parallel-plate waveguide.

declined from the normal. This operation of the metamirror was examined at the operating frequency 5 GHz with full-wave simulations and experimental set-up shown in Fig. 5. A single row of the elements was placed between the plates of a parallel-plate waveguide with the following dimensions: the sizes along the y- and z-axes are, respectively, 80 cm and 90 cm, and the height equals to $a = 15$ mm. Since the elements of the metamirror can be considered as coupled vertical electric and horizontal magnetic dipoles, based on the image principle, a single row of the elements placed in the waveguide emulates a two-dimensional structure infinite in the x-direction. A vertical coaxial source that generates a cylindrical wave with the electric field along the x-axis was used as the feed in both simulations and experiment. The initial location of the feed was in the focal point of the metamirror on the z-axis. On the edges of the waveguide the boundary conditions of a perfectly matched layer were applied in simulation and the absorbing material blocks (10 cm width) were placed in experiment to avoid parasitic reflections. The source was displaced laterally from the focal point of the metamirror along the y-axis at 5 mm and 10 mm, which corresponds to the defocusing angles $\theta_d = 7°$ and $\theta_d = 16°$ received in the previous section. The simulated results for these two cases are shown in Figs. 6a and 6c. Fig. 7 shows the radiation patterns of the metamirror in the yz-plane.

The experimental set-up was slightly more complex. In the bottom plate of the waveguide a copper mesh (25×35 cm) was embedded. Using a movable coaxial probe positioned under the mesh, it is possible to measure the spatial distribution of the x-component of the electric field inside the waveguide. To determine the distribution of the reflected fields from the metamirror, two sets of measurements are needed. First, the empty waveguide was analysed to obtain the field distribution of the incident wave. In the second set of measurements with the metamirror placed inside the waveguide, the total fields were measured. The reflected fields distribution was

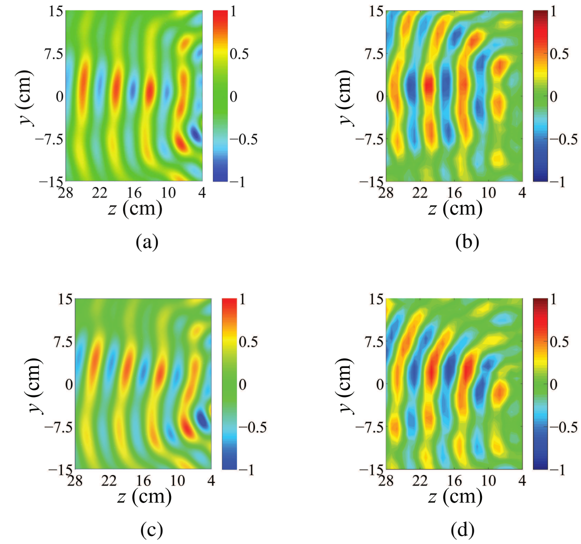

Fig. 6. The electric field distributions of the wave reflected from the metamirror. The feed and the metamirror are positioned at $z = 3.9$ cm and $z = 0$ cm, respectively. Plots (a) and (c) depict the simulated field distributions for the cases when the feed was displaced by $\theta_d = 7^\circ$ and $\theta_d = 16^\circ$, respectively. Plots (b) and (d) show the corresponding measured field distributions.

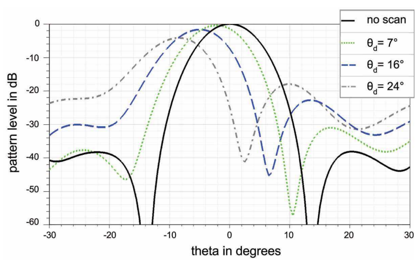

Fig. 7. Simulated scanned beam pattern for the metamirror with the subtended angle $\theta_0 = 77^\circ$ ($f/D = 0.12$).

found by subtracting the incident fields from the total ones. The measured field distribution of the reflected wave from the metamirror for the two cases of feed displacement are presented in Figs. 6b and 6d. The numerical data obtained in simulations are summarized in Table II

Defocusing angle θ_d, deg	Lateral displacement from the focal spot, mm	Scanned beam angle (simulation/ experiment) θ_b, deg	BDF (simulation/ experiment)	Main beam level, dB
7	5	3.0 / 4.4	0.43 / 0.63	16.1
16	11	6.0 / 7.0	0.38 / 0.44	14.7

TABLE II
THE BEAM STEERING DUE TO THE LATERAL FEED-DISPLACEMENT

As it can be seen, the scanned angles of the main beam in the experiment are well correlated with the corresponding values achieved through full-wave simulations. In addition, we can conclude that despite of the sub-wavelength focal length, the scanning characteristics of the studied metamirror are at the same level as those of comparable reflectarrays. Comparison with the results of [6] shows that the scanning performance of the metamirror is on par with the comparable reflectarray.

III. Conclusion

We have examined novel metasurface-based reflectors through their two reciprocal functions: the scanning ability at feed displacements and the focusing ability for incident waves deviating from the main-beam direction. Although, a reflector with a sub-wavelength focal length could have been expected to be impractical due to its potentially strong sensitivity to the feed position, both the simulated and measured results of the considered extremely short-focus metamirrors reveal their modest but acceptable for many applications scanning properties. Thus, transparent outside the operational frequency range metamirrors can be used in various applications, in particular for satellites, for radioastronomy and together with solar energy harvesting systems.

Acknowledgment

This work was supported by Academy of Finland (project 287894).

References

[1] Y. Ra'di, V. S. Asadchy, and S. A. Tretyakov, "Tailoring reflections from thin composite metamirrors", *IEEE Trans. Antennas Propagat.*, vol. 62, no. 7, pp. 3749–3760, July 2014.

[2] V. S. Asadchy, Y. Ra'di, J. Vehmas, and S. A. Tretyakov, "Functional metamirrors using bianisotropic elements", *Physical Review Letters*, vol. 114, no. 9, pp. 0955031–0955035, March 2015.

[3] V. S. Asadchy, S. N. Tcvetkova, Y. Ra'di, and S. A. Tretyakov, "Highly efficient frequency-selective reflectarrays based on sub-wavelength elements", in *36th ESA Antenna Workshop on "Antennas and RF Systems for Space Science"*, Noordwijk, The Netherlands, Oct. 6–9, 2015.

[4] Y. T. Lo, "On the beam deviation factor of a parabolic reflector", *IRE Transactions on Antennas and Propagation*, vol. 8, no. 3, pp. 347–349, 1960.

[5] M. Zimmwrman, S. W. Lee, B. Housmand, Y. Rahmat-Samii, and R. Acosta, "A comparison of reflector antenna design for a wide-angle scanning", *NASA Technical Memorandum 101459*, February 1989.

[6] S. R. Rengarajan, "Scanning and defocusing characteristics of microstrip reflectarrays", *IEEE Antennas Wireless Propag. Lett.*, vol. 9, 2010.